

Supporting Information

Two-dimensional Ferroelastic Ferromagnet NiOX (X = Cl, Br) with Half-Metallicity and High Curie Temperature

Gang Xiao ^a, Wen-Zhi Xiao ^{a*}, Ying-Xue Feng ^a, Qing-Yan Rong ^a, Qiao Chen ^a

^a School of Computational Science and Electronics, Hunan Institute of Engineering,
Xiangtan 411104, China

➤ The search process of the evolutionary algorithm ^[1]:

The global minimum energy configuration for NiOX (X = F, Cl, Br, I) binary compounds with 3-12 atoms in each unit cell and an element ratio of 1:1:1 is obtained using the Evolutionary Algorithm (EA) within the USPEX (Universal Structure Predictor: Evolutionary Xtallography) software. When iterating the population, the initial population size is set to 90, the population size of each subsequent generation is 40, the population generation is 60 generations, and the first 50% of the energy of the current generation is retained to produce offspring. During evolution, 50% of the population is generated by inheritance, 30% is randomly generated by space group symmetry, 10% by lattice mutation and 10% by soft mode mutation. A simulation is stopped early if the optimal structure remains unchanged for 20 generations.

➤ Calculations of Young's modulus and Poisson's ratio for NiOX monolayer:

We calculated the orientation-dependent Poisson's ratio ν and Young's modulus Y by using the following equations:

$$\begin{cases} Y(\theta) = \frac{Y_{zz}}{\cos^4 \theta + d_2 \sin^2 \theta \cos^2 \theta + d_3 \sin^4 \theta} \\ \nu(\theta) = \frac{\nu_{zz} \cos^4 \theta - d_1 \sin^2 \theta \cos^2 \theta + \nu_{zz} \sin^4 \theta}{\cos^4 \theta + d_2 \sin^2 \theta \cos^2 \theta + d_3 \sin^4 \theta} \end{cases} \quad (5)$$

where d_1 , d_2 , d_3 , Y_{zz} , and ν_{zz} are elasticity-constant-related variables described in detail

*Corresponding author: xiaowenzhi@hnie.edu.cn

in the references^[2, 3, 4].

➤ **The calculations of the exchange coupling parameters:**

To estimate the Curie temperature (T_C), the exchange coupling parameters were extracted according to the spin model Hamiltonian expressed as:

$$H = H_0 - J_1 \sum_{\langle ij \rangle} \vec{S}_i \cdot \vec{S}_j - J_2 \sum_{\langle\langle ij \rangle\rangle} \vec{S}_i \cdot \vec{S}_j - J_3 \sum_{\langle\langle\langle ij \rangle\rangle\rangle} \vec{S}_i \cdot \vec{S}_j - A \sum_i \vec{S}_i^e \cdot \vec{S}_i^e$$

where J_1 , J_2 , and J_3 are the first, second, and the third nearest neighboring exchange parameters, respectively; The subscripts $\langle ij \rangle$, $\langle\langle ij \rangle\rangle$, and $\langle\langle\langle ij \rangle\rangle\rangle$ denote summations between the corresponding neighbors; $\vec{S}_{i/j}$ is the spin vector at the i/j site; A is anisotropy energy parameter of each magnetic ion and \vec{S}_i^e is the spin component along the easy magnetic axis; The energies of the four potential magnetic configurations (Figure 1(a)) were written as:

$$\begin{cases} E_{\text{FM}} = E_0 - N \frac{S^2}{2} (2J_2 + 4J_1 + 2J_3) - NAS^2 \\ E_{\text{AMF}} = E_0 - N \frac{S^2}{2} (2J_2 - 4J_1 + 2J_3) - NAS^2 \\ E_{\text{AFM1}} = E_0 - N \frac{S^2}{2} (2J_2 + 0J_1 - 2J_3) - NAS^2 \\ E_{\text{AFM2}} = E_0 - N \frac{S^2}{2} (-2J_2 + 0J_1 + 2J_3) - NAS^2 \end{cases}$$

where E_{FM} , E_{AMF} , E_{AFM1} , and E_{AFM2} correspond to the energies of a $2 \times 2 \times 1$ supercell for different configurations, the N ($= 8$) represents the number of Ni atoms in a $2 \times 2 \times 1$ supercell, E_0 is the energy of the ground state without dependence on the magnetic configuration. The factor of $1/2$ in the energy expression is to avoid double counting. Since each Ni carries a magnetic moment of about $1.0 \mu_B$, the S therefore is treated as $1/2$ in our calculations. We then can estimate J_1 , J_2 , and J_3 from the following equations for NiOCl and NiOBr monolayers.

$$\begin{cases} E_{\text{FM}} + E_{\text{AMF}} - 2E_{\text{AFM2}} = -N \frac{S^2}{2} 8J_1 \\ E_{\text{FM}} - E_{\text{AMF}} = -N \frac{S^2}{2} 8J_2 \\ E_{\text{FM}} + E_{\text{AMF}} - 2E_{\text{AFM1}} = -N \frac{S^2}{2} 8J_3 \end{cases}$$

For the NiOF monolayer case, we considered four potential magnetic configurations as shown in Fig. S5(a). Therefore, the calculated J_1 , J_2 , and J_3 correspond to J_2 , J_1 , and J_3 , respectively, for the NiOCl or NiOBr cases.

- **Table S1.** Optimized structural properties of three different 2D NiOCl crystal structures. a , b and c are the lattice constants. Atomic positions are the group Wyckoff positions for each independent atoms in fractional coordinates. All the parameters are calculated by GGA+U (U = 3.3 eV) method.

Structure	LNS	1T	Tetragonal
Space group	Pmmn (#59)	P3m1 (#156)	P4/nmm (#129)
a (Å)	3.057	3.105	3.660
b (Å)	3.715	3.105	3.660
c (Å)	20.00	20.00	20.00
Positions	O (0.5, 0.5, 0.521) Cl (0.5, 0.5, 0.375) Ni (0.0, 0.5, 0.457)	O (2/3, 1/3, 0.442) Cl (0.0, 0.0, 0.558) Ni (1/3, 2/3, 0.477)	O (0.0, 0.0, 0.0) Cl (0.0, 0.5, 0.637) Ni (0.0, 0.5, 0.527)

➤ **Table S2.** Relative energies ΔE ($=E_{\text{AFM0}}-E_{\text{FM}}$) (meV), magnetic moments MM (μ_{B}) per unit cell, and conductivity with GGA+U (U =3.3 eV) and HSE06 for NiOX (X = F, Cl, Br) monolayers, respectively.

	GGA+U ΔE	HSE06 ΔE	GGA+U MM	HSE06 MM	GGA+U conductivity	HSE06 conductivity
<i>NiOF</i>	57.8	57.3	2.00	2.00	Half-metal	Half-metal
<i>NiOCl</i>	57.4	54.6	2.00	2.00	Half-metal	Half-metal
<i>NiOBr</i>	56.3	52.7	2.00	2.00	Half-metal	Half-metal

➤ **Figure S1**

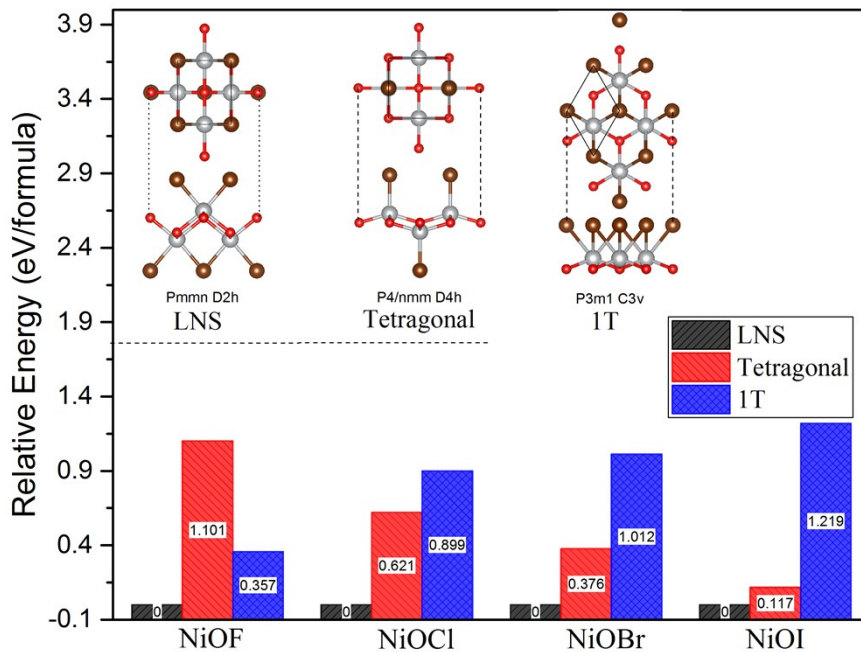


Figure S1. Calculated relative energies (eV per chemical formula) which refer to that of the most stable 2D NiOX (X = F, Cl, Br) structure in the lepidocrocite-type (LNS) phase. The inset shows the corresponding top and side views of various configurations that are identified as the three most stable phase in energy.

➤ **Figure S2**

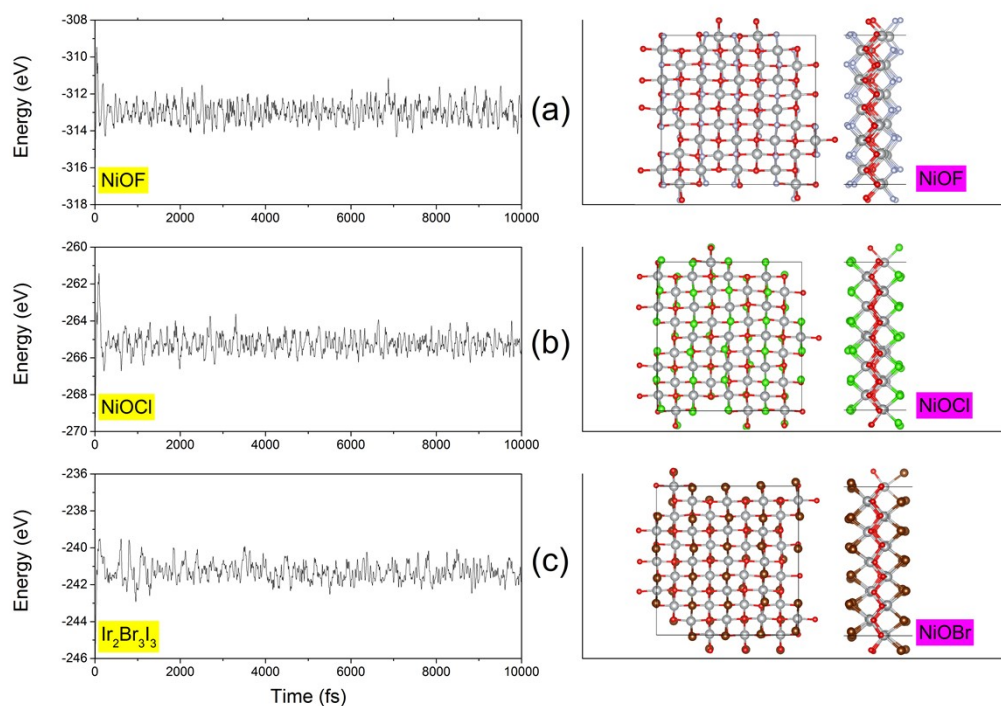


Figure S2. Total energy as a function of time during *ab initio* molecular dynamics simulation at 350 K for (a) NiOF, (b) NiOCl, and (c) NiOBr monolayers. The top views of the snapshot of monolayers NiOX are also shown after 10 ps in the AIMD simulation.

➤ **Figure S3**

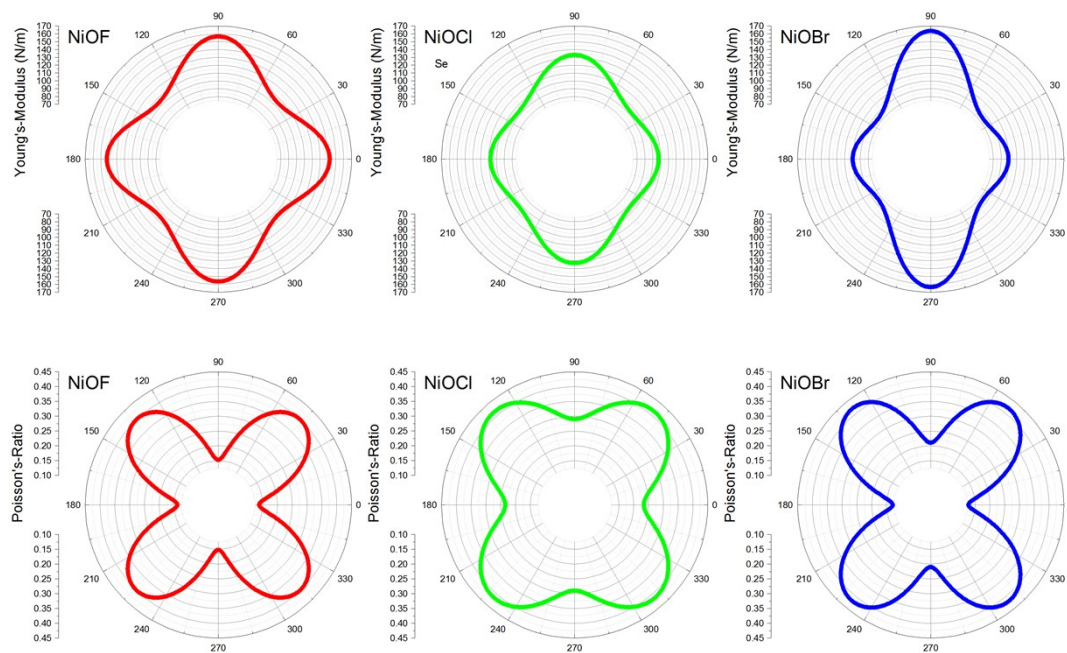


Figure S3. Calculated orientation-dependent Young's modulus $Y(\theta)$ and Poisson's ratio $\nu(\theta)$. The angle θ measured clockwise from the referent x -axis.

➤ **Figure S4**

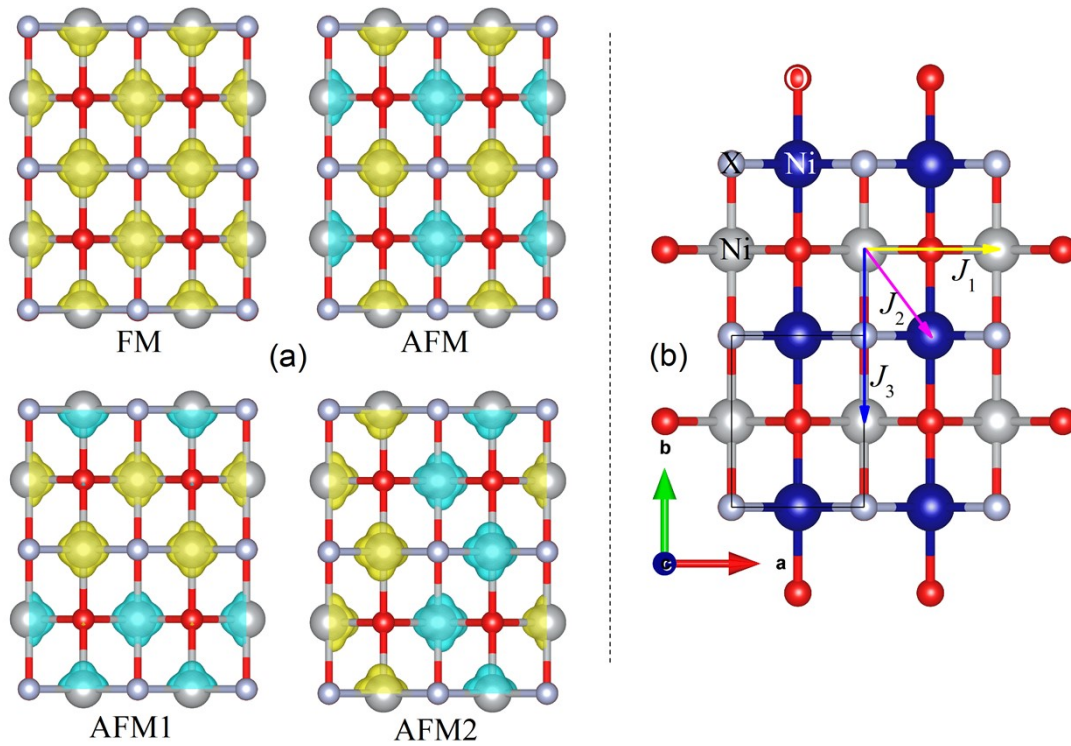


Figure S4. (a) Top views of the $2 \times 2 \times 1$ supercell with different magnetic orders, including possible FM, AFM, AFM1, and AFM2 magnetic configurations. The yellow and green isosurfaces with value of $0.03 e/\text{\AA}^3$ denote two opposite spin orientations. (b) The schematic diagram for the exchange interaction constants: J_1 , J_2 , and J_3 for the NiOF monolayer. They are the nearest, next nearest, and third nearest magnetic exchange interaction parameters, respectively.

➤ **Figure S5**

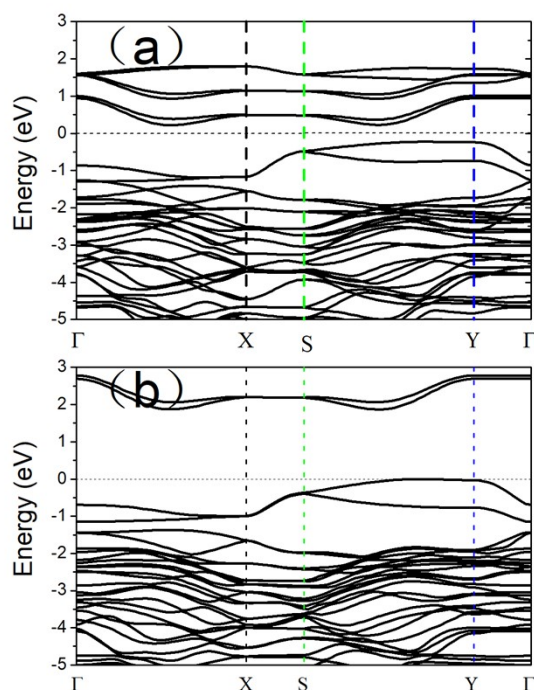


Figure S5. Electronic band structures of the NiOF monolayers in AFM state obtained from (a) GGA+U and (b) HSE06 methods.

➤ **Figure S6**

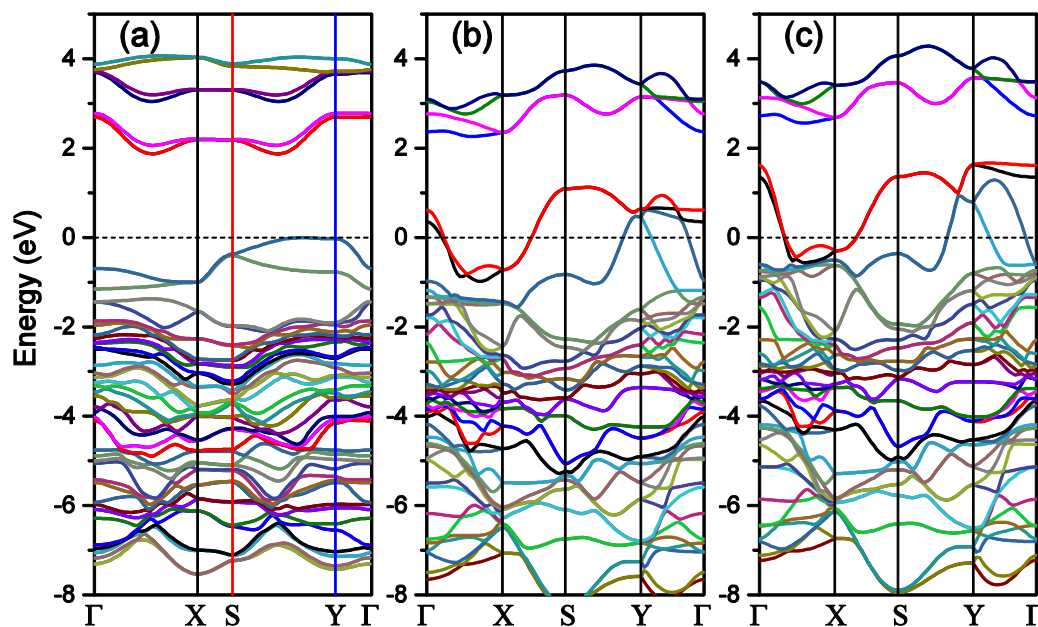


Figure S6. The Electronic band structures of the (a) NiOF, (b) NiOCl, (c) NiOBr monolayers in their ground state at HSE06 level with SOC. A dashed line at 0.0 eV denotes the Fermi level.

➤ **Figure S7**

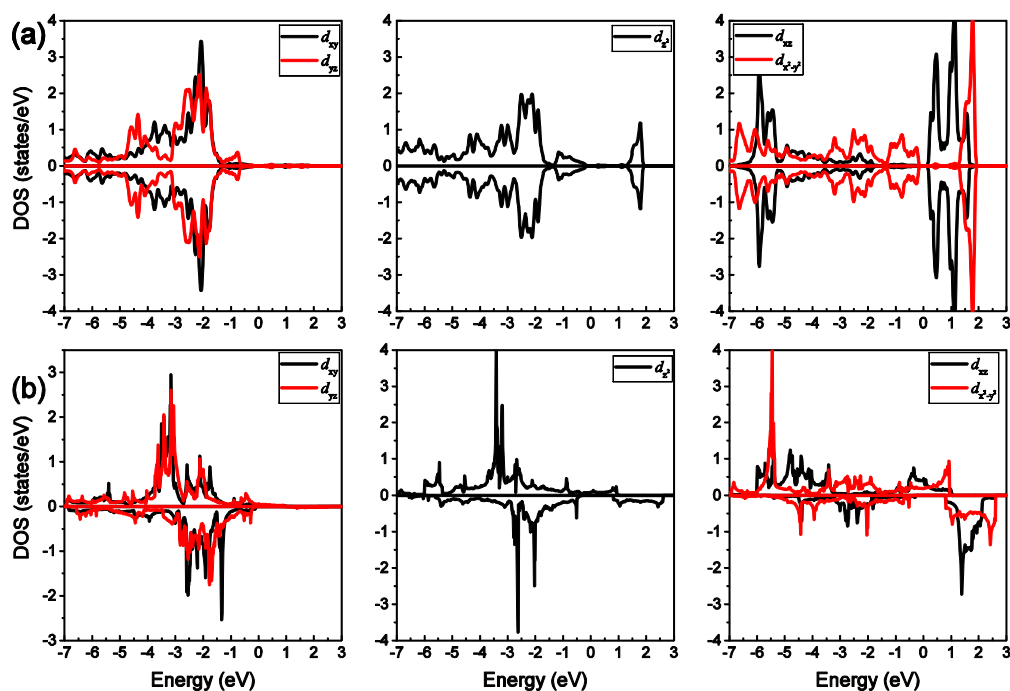


Figure S7. The projected density of states (PDOS) of Ni-3d orbitals of the (a) NiOF and (b) NiOBr in their ground state at the GGA+U level. The Fermi level is denoted by a dashed line at 0.0 eV.

➤ **Figure S8**

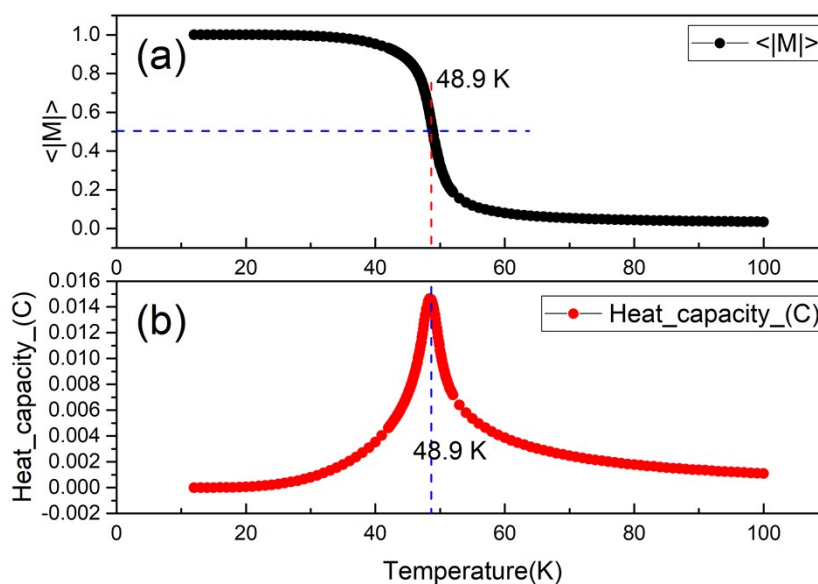


Figure S8. The Monte Carlo simulated (a) normalized magnetization and (b) specific heat as a function of temperature using the Heisenberg model for CrI_3 monolayers.

-
- ¹ A. O. Lyakhov, A. R. Oganov, H. T. Stokes, Q. Zhu, New developments in evolutionary structure prediction algorithm USPEX, *Comp. Phys. Comm.*, 2013,**184**, 1172.
- ² L. Wang, A. Kutana, X. Zou and B. I. Yakobson, Electro-mechanical anisotropy of phosphorene. *Nanoscale*, 2015, 7, 9746–9751.
- ³ H. Wang, X. Li, P. Li, J. Yang, δ -Phosphorene: a two dimensional material with a highly negative Poisson's ratio. *Nanoscale*, 2017, **9**(2), 850-855.
- ⁴ E. Cadelano, P. L. Palla, S. Giordano, L. Colombo, Elastic properties of hydrogenated grapheme. *Phys. Rev. B*, 2010, **82**(23), 235414.